X-ray emission from the cluster around E 1821+643

R. D. Saxton, M. A. Barstow, M. J. L. Turner,
O. R. Williams, G. C. Stewart, T. Kii

ESLAB 97 057

accepted by MNRAS

X-RAY EMISSION FROM THE CLUSTER AROUND E 1821+643

ABSTRACT

We report the first unambiguous detection of X-ray emission from the cluster of galaxies surrounding the radio-quiet QSO E 1821+643 . *ROSAT* PSPC observations show that the cluster is highly luminous, $L_x \sim 10^{45}$ ergs s^{-1}, as would be expected from the high Abell richness class (≥ 2) seen in optical studies. The cluster is expected to contribute an iron line of apparent equivalent width 20–142 eV to the integrated spectrum.

X-RAY EMISSION FROM THE CLUSTER AROUND E 1821+643

R.D.Saxton[1], M.A.Barstow[2], M.J.L.Turner[2], O.R.Williams[3], G.C.Stewart[2], T.Kii[4]

[1]VEGA, ISO Science Operations Centre, Astrophysics division of ESA,
Villafranca del Castillo, Apartado 50727, 28080 Madrid, Spain.
[2]Department of Physics and Astronomy, University of Leicester,
University Road, Leicester LE1 7RH, UK.
[3]Astrophysics Division, ESTEC, Keplerlaan 1, Postbus 299,
2200 AG Noordwijk, The Netherlands.
[4]Institute of Space and Astronautical Science, 3-1-1, Yoshinodai,
Sagamihara, Kanagawa 229, Japan.

April 11, 1997

ABSTRACT

We report the first unambiguous detection of X-ray emission from the cluster of galaxies surrounding the radio-quiet QSO E 1821+643 . *ROSAT* PSPC observations show that the cluster is highly luminous, $L_x \sim 10^{45}$ ergs s^{-1}, as would be expected from the high Abell richness class (≥ 2) seen in optical studies. The cluster is expected to contribute an iron line of apparent equivalent width 20–142 eV to the integrated spectrum.

Keywords: galaxies: clustering - galaxies: X-rays - quasars -
galaxies:individual:E 1821+643

1 INTRODUCTION

Optical studies of the QSO E 1821+643 have revealed that it lies near the centre of a cluster of galaxies (Schneider *et al.* 1992) which, with an Abell richness class ≥ 2 (Lacy, Rawlings & Hill 1992), is among the richest known. E 1821+643 at a redshift of 0.297 and luminosity, $L_x \sim 10^{46}$ ergs s^{-1} ($H_0 = 50, q_0 = 0.5$) is among the brightest QSOs in the sky and has been observed by many X-ray missions since being listed as H 1824+644 in the *HEAO-1/A2* high-energy experiment catalogue (Marshall *et al.* 1979). *EXOSAT* observed the source seven times during 1984 and 1985 and found the medium-energy (2–10 keV) flux to be almost constant while the low-energy flux varied on a timescale of months (Warwick, Barstow & Yaqoob 1989). The size of the point spread function (PSF) of the LE telescope and the relatively high detector background made it impossible to see any extended emission from a low surface brightness cluster in these observations, even though an effective exposure time of 60ks was available by mosaicing the images.

Ginga detected a strong iron emission line with an equivalent width of 275 ± 105 eV in the spectrum of the QSO (Kii *et al.* 1991). This is by far the most luminous active galaxy in which such a feature has been seen; the only comparable source, 3C 273, has an iron line of equivalent width $\lesssim 50$ eV (Turner *et al.* 1990). Kii *et al.* estimated the possible contribution to the line by diffuse intra-cluster gas emission, concluding that it could provide up to 110 eV. This left the possibility that the iron line equivalent width intrinsic to the QSO could be as low as 60 eV, which would make it unremarkable.

Here we report on two *ROSAT* observations of the X-ray emission from the cluster and study its effect on the equivalent width inferred for the QSO iron line.

2 Observations and Data Analysis

E 1821+643 has been seen serendipitously in two pointed *ROSAT* PSPC observations made with the Boron filter of the nearby white dwarf WD 1821+643 (K1-16) (Table 1). A visual inspection of the data suggests that the emission is extended. To test this hypothesis, a radial profile of the source counts at approximately 1 keV (chns. 70 – 129)

has been compared with a standard on-axis PSF generated from a three-component fit to several on-axis point sources (Hasinger *et al.* 1992a). The comparison was made at 1 keV because the PSF is well determined at this energy (Hasinger *et al.* 1992b) and because there is no contribution expected from the nearby white dwarf. Typically all the photospheric flux from a very hot planetary nucleus central star like K1-16 falls below the Carbon K_α absorption edge of the PSPC window at 0.28 keV (see e.g. the discussion in Warwick, Barstow & Yaqoob 1989). However, coronal X-ray emission has been detected from the white dwarf KPD 0005+5106 (Fleming, Werner & Barstow 1993) which could, if present in K1-16, extend the X-ray spectrum up to higher energies than otherwise expected. Pulse height distributions for both K1-16 and E 1821+643 have been obtained from the *ROSAT* data, using a restricted extraction radius to minimise contamination of one source by the other (Figure 1). A comparison of these confirms that the white dwarf spectrum is indeed extremely soft compared with the QSO and makes a negligible contribution to the total flux above 0.3 keV.

Inspection of the image from the first observation shows that the extended emission is approximately circular (Figure 2). A fit of the radial profile predicted by the PSF to that of the QSO yields a poor result for both observations, χ^2_r=14.5 and 3.9 respectively. Only data taken with a nominally perfect attitude solution were used in this analysis.

The background was taken from a source free area, away from the extended central source but within the central ring of the PSPC window support structure. This was corrected for the instrument vignetting at 1 keV before being subtracted from the image.

As a further test, a Boron filter observation of a source with a similar spectrum and signal to noise ratio as E 1821+643 , the QSO PG 1426+015, was obtained from the *ROSAT* data archive (Sembay 1993) and shown to be a good fit to the PSF (χ^2_r=1.2). The radial profile fits are shown in Figure 3.

2.1 Cluster deprojection

The X-ray emission from clusters often follows a radial distribution which can be represented by a King profile (King 1962),

$$C(r) = C_0(1 + \frac{r^2}{r_c^2})^{0.5-3\beta} \quad (1)$$

where C_0 is the surface brightness at the centre of the cluster, r_c is the core radius of the cluster and β is a slope parameter.

In an attempt to find the radial distribution of the cluster emission, the radial profile of the QSO system from the first, higher signal-to-noise, observation was modelled with a King profile and a point source.

$$P(r) = Q\Psi(r) + C'(r) \quad (2)$$

where $P(r)$ is the surface brightness at radius r, Q is the QSO brightness, Ψ is the PSF and C' is the convolution of the King profile with the PSF.

The cluster parameters, β and r_c were varied and gave best-fit values of $\beta = 0.70^{+0.15}_{-0.08}$ and $r_c = 0.42^{+0.36}_{-0.24}$ arcminutes, or 139^{+119}_{-79} kpc, at 90% confidence. Confidence contours for these parameters are shown in Figure 4, the best fit model ($\chi^2_r = 1.0$) and the residuals are given in Figure 5.

Excess emission, attributed to a cooling flow, is seen in the central regions of most X-ray clusters (e.g. Fabian *et al.* 1986). Confusion with the dominant point source in this case makes it impossible to search for a cooling flow with this data given the expected size of the cooling radius.

2.2 Spectral fits

A spectrum of the cluster was produced by sorting data between channels 70 and 129 (outside the white dwarf range) from an annulus of inner radius 1 arcminute and outer radius 3 arcminutes centred on the QSO. To remove the residual effects of the QSO in this area, the background subtracted counts within the inner arcminute were multiplied by the ratio of counts in the two areas seen in the PG 1426+015 observation. This ratio was

determined at 6 different channel ranges from 70 to 129 and has a mean of (0.009). To check that these values were representative, the process was repeated on a further source, 3C273, extracted from the data archive. This gave a similar set of ratios with a mean of (0.013). The normalised QSO counts were then subtracted from the cluster spectrum. The resultant spectrum was background subtracted using a circular area of blank sky outside the cluster but within the central ring of the PSPC window support structure.

The signal-to-noise ratio of the subtracted spectrum is too low to constrain spectral fit parameters but the data may be used to normalise potential models. The spectrum was fitted with a Raymond-Smith model, over the range of temperatures normally seen in clusters, and with a column density of 3.4×10^{20} cm^{-2}. This value for the galactic absorption towards E 1821+643 was determined by a new mapping of 21 cm emission towards *ROSAT* AGN by Jodrell Bank (Pedlar 1991, private communication). The 2–10 keV flux of each model was found by extrapolation and is used later in Table 3 to calculate the flux from the total cluster.

During the *ROSAT* survey in 1990, a quasi-simultaneous measurement of E 1821+643 was made with *Ginga* . The *Ginga* spectrum can be well fit with a model of a power law plus an iron line and galactic absorption (Table 2). The parameters are compatible with those seen in the observations of 1987 and 1988 (Kii *et al.* 1991) but both the 2–10 keV flux and the flux in the iron line appear to have fallen by $\sim 50\%$. The observed equivalent width of the iron line is 208^{+99}_{-82} eV similar to that seen in the earlier observations. Unfortunately there is a discrepancy in the normalisation of the *ROSAT* and *Ginga* spectra at 2 keV in this observation (see Walter *et al.* 1994 for a discussion) suggesting that the hard component may have varied during the 40 day *ROSAT* survey observation. This makes a fit of the combined *ROSAT* and *Ginga* spectrum questionable, however the *Ginga* spectrum alone may be used to place upper limits on the thermal flux from a cluster. The *Ginga* spectrum was fitted with a power law plus a narrow line to model the QSO emission, and a Raymond-Smith, with metal abundance set to 0.3 times solar to model the cluster emission, for a range of cluster temperatures between 3 and 12 keV. The 90% upper limit for the cluster flux is used to derive the upper error bars on the total cluster flux given in Table 3 and plotted in Figure 6.

3 RESULTS

3.1 The Cluster

The range of King profiles allowed by Figure 4 includes values similar to those seen in other clusters where core radii range from $\sim 100-600$ kpc (e.g. Jones and Forman 1984).

The ratio of the total cluster flux to that which we measure between 1 and 3 arcminutes is dependent on the radial profile. It can be derived by convolving the cluster radial profile with the PSF and is given in Table 4 for the range of acceptable fits. The ratio is $3.8^{+1.9}_{-1.0}$ at 90% confidence. With this ratio the total flux from the cluster may be calculated and is plotted as a function of temperature in Figure 6.

The *Ginga* observation puts a limit on the total flux which can come from the cluster and this is a stronger constraint than the ratio upper limit of 5.7 for all temperatures (see Figure 6). Table 3 shows the 2-10 keV flux inferred for the cluster, with the upper error bar being the maximum permitted by the *Ginga* observation and the lower error bar being the lower limit of the flux measured from the *ROSAT* observation multiplied by 2.8.

The X-ray and bolometric luminosities of the cluster for each temperature are given in Table 3. Bolometric correction factors were calculated by extrapolating the X-ray spectrum between 1.0×10^{-4} and 1.0×10^{4} keV (in the manner of Edge 1989).

Work by Edge & Stewart (1991a) has indicated a strong correlation between cluster luminosity and temperature with $L_{bol} \simeq 10^{43} \times T^{2.6}$ ergs s^{-1}. If the cluster gas were at a temperature of 3–5 keV it would be several times too luminous to conform to this relationship, however, a cluster temperature of 7–12 keV would fit the relation. The high Bahcall Galaxy Density, $N_{0.5} = 59 \pm 10$ (Lacy, Rawlings & Hill 1992), is also more consistent with a high temperature, from relationships seen in nearby clusters (Edge & Stewart 1991b).

3.2 The QSO Iron Line

The iron line flux expected from the cluster has been calculated using the inferred total cluster flux and assuming an Fe abundance of 0.2–0.4 solar (representative of the range seen in clusters; Hatsukade 1989) (Table 3). This gives a line strength of between 0.6 and 4.2 $\times 10^{-5}$ photons cm^2 s^{-1}.

The Iron line flux from the system as a whole was $6.2 \pm 2.1 \times 10^{-5}$ photons cm^{-2} s^{-1} in the combined 1987 and 1988 observations of the QSO (Kii *et al.* 1991), corresponding to an observed equivalent width of 210 ± 80 eV. Therefore, depending on the temperature and iron abundance, the cluster will contribute between 20 and 142 eV of this observed line.

The cluster also provides a significant fraction of the continuum emission from the system. The equivalent width of the iron line from the QSO alone can be calculated by subtracting the cluster emission from the total system and is given as a function of cluster temperature in Table 5. The lower limit for the observed equivalent width of the QSO iron line at 90% confidence is 31 eV.

4 DISCUSSION

We have shown that the cluster associated with the QSO E 1821+643 makes a significant contribution to the 2–10 keV flux of the total system. Depending on the cluster temperature, between 10 and 50% of the medium-energy flux detected by *Ginga* during the 1987 and 1988 observations will have come from the cluster. Since the majority of the cluster emission comes from within one arcminute of the centre of the QSO, any analysis should take the cluster into account.

As an example, if we assume that the cluster has a temperature of 7 keV, an iron abundance of 0.3 and use the best fit to the radial profile, ratio=3.8, then the 2–10 keV flux from the cluster would be $\sim 7 \times 10^{-12}$ ergs cm^{-2} s^{-1} and the iron line flux would be $\sim 2.3 \times 10^{-5}$ photons cm^{-2} s^{-1}. Meaning that in 1987/1988 the QSO flux was $\sim 1.3 \times 10^{-11}$ ergs cm^{-2} s^{-1} and the QSO iron line was $\sim 3.9 \pm 2.1 \times 10^{-5}$photons cm^{-2} s^{-1} giving an

observed equivalent width for the QSO of $\sim 240 \pm 130$ eV. In the 1990 observation the QSO flux would be $\sim 6 \times 10^{-12}$ ergs cm^{-2} s^{-1} and the equivalent width $\sim 270 \pm 280$ eV. If this was the case then the QSO flux would have varied by a factor of 2 between the observations. The presence of the cluster may help to explain why the medium-energy flux from E 1821+643 has appeared to be relatively constant over the years.

The cluster in which the QSO is situated is itself an interesting object. The very high luminosity, $L_{bol} \geq 3 \times 10^{45}$ ergs s^{-1}, would place the cluster at the very extreme of the local cluster luminosity function (Edge *et al.* 1990). The strong negative evolution observed in the number density of the most luminous clusters (Edge *et al.* 1990; Gioia 1990) suggests a reduction in the space density of such objects by a factor of ~ 5 by a redshift of 0.3, making this cluster an even rarer example and suggesting that it is indeed an extremely massive object. The X-ray evidence is supported by the high galaxy richness. A definitive measurement of the X-ray temperature will be important in understanding the evolutionary status of the cluster gas. The contamination by the strong central source and the limited spatial extent will require the high resolution of instruments such as JET-X, XMM and AXAF for this to be achieved.

We also note that such a luminous cluster would reasonably be expected to have a cooling flow of up to several hundred solar masses per year. We note that many of the higher luminosity AGN at these and higher redshifts are apparently centrally located within clusters with significant cooling flows (e.g. Crawford & Fabian 1989).

5 CONCLUSIONS

We have shown that the cluster of galaxies surrounding the QSO, E 1821+643 , is a strong X-ray emitter with a luminosity of $L_x \sim 10^{45}$ergs s^{-1}. Depending on the temperature and iron abundance of the cluster, the observed equivalent width of the iron line intrinsic to the QSO may be as low as 31 eV or may even be higher than previously thought. An accurate measurement of the cluster parameters is needed to resolve this question.

6 ACKNOWLEDGMENTS

The authors would like to thank Alan Pedlar for measuring the galactic absorption towards E 1821+643 and Andy Pollock for useful discussions. The helpful comments of the anonymous referee are gratefully acknowledged. GCS and MAB acknowledge support of PPARC in the form of advanced fellowships.

REFERENCES

Crawford, C.S., Fabian, A.C., 1989, MNRAS, 239, 219

Edge, A.C., 1989, Ph.D. thesis, University of Leicester.

Edge, A.C., Stewart, G.C., 1991a, MNRAS, 252, 414

Edge, A.C., Stewart, G.C., 1991b, MNRAS, 252, 428

Edge A.C., Stewart, G.C., Fabian, A.C. Arnaud, K.A., 1990, MNRAS, 245, 559

Fabian, A.C., Arnaud, K.A., Nulsen, P.E.J. Mushotzky, R.F., 1986, ApJ, 305, 9

Fleming, T.A., Werner, K., Barstow, M.A., 1993, ApJ, 416, L79

Gioia, I.M., Henry, J.P., Maccacaro, T., Morris, S.L., Stocke, J.T. Wolter, A., 1990, ApJ, 356, L35

Hasinger, G, Turner, T.J., George, I.M., Boese, G, 1992a. OGIP calibration memo CAL/ROS/92-001 published in 'Legacy II'

Hasinger, G, Turner, T.J., George, I.M., Boese, G, 1992b. OGIP calibration memo CAL/ROS/92-001a

Hatsukade, I., 1989, Ph.D. thesis, Osaka University (ISAS Res. Note, 435)

Jones, C., Forman, W., 1984, AJ, 276, 38

Kii et al. 1991, ApJ, 367, 455

King 1962, AJ, 67, 471

Lacy, M., Rawlings, S., Hill, G.J., 1992, MNRAS, 258, 828

Marshall, F. E., Boldt, E.A., Holt, S.S., Mushotsky, R.F., Pravdo, S.H., Rotschild, R.E., Serlemitsos, P.J., 1979, ApJS, 40, 657

Schneider, D.P., Bahcall, J.N., Gunn, J.E., Dressler, A., 1992, AJ, 103, 1047

Sembay 1993, Starlink MUD 143, "The UK *ROSAT* Data Archive - user guide".

Turner, M.J.L. et al., 1990, MNRAS, 244, 310

Walter, R., Orr, A., Courvoisier, T.J.-L., Fink, H.H., Makino, F., Otani, O., Wamsteker, W., 1994, A&A, 185, 119

Warwick, R.S., Barstow, M.A., Yaqoob, T., 1989, MNRAS, 238, 917

Table 1: *ROSAT* observations of E 1821+643

Observation date	Exposure time (s)	Count rate (chn:70-199)	
		0'–1'[a]	1'–3'[b]
22 February 1991	7919[c]	0.42 ± 0.01	0.05 ± 0.01
8 December 1992	2896	0.47 ± 0.01	0.04 ± 0.02

[a]The total count rate within one arcminute of the source centre after background subtraction.

[b]The count rate between one and three arcminutes from the source centre after background subtraction and with the contribution from the point source removed.

[c]After correction for attitude errors (originally 8650s).

Table 2: Power law plus emission line plus absorption spectral fits to *Ginga* observations of E 1821+643

	F_x (2–10 keV)		Line Energy	Line Flux	
Observation[a]	(10^{-11} ergs cm^{-2} s^{-1})	α	(keV)	(photons cm^{-2} s^{-1})	χ^2/ν
May 1987[b]	2.1 ± 0.3	0.91 ± 0.03	5.13 ± 0.32	$5.8(\pm 2.5) \times 10^{-5}$	34/21
Sep 1988[b]	1.9 ± 0.3	0.87 ± 0.05	5.21 ± 0.24	$6.9(\pm 3.4) \times 10^{-5}$	14/21
Oct 1990	1.3 ± 0.3	0.87 ± 0.06	4.85 ± 0.36	$4.5(\pm 2.3) \times 10^{-5}$	36/42

[a]To provide a direct comparison between the 3 observations, the column density has been set to the galactic value used in Kii *et al.* 1991 (4.0×10^{20} cm^{-2}) in all of the fits.

[b]Taken directly from Kii *et al.* .

Table 3: Properties of the cluster surrounding E 1821+643

Temperature (keV)	F_X^a	L_X^{bc}	Bolometric correction	L_{bol}^{dc}	Iron line flux[e]
3	2.25 ± 0.35	0.95 ± 0.15	3.4	3.2 ± 0.5	1.05 ± 0.45
4	3.75 ± 1.15	1.6 ± 0.5	2.7	4.3 ± 1.3	1.85 ± 1.05
5	5.25 ± 1.85	2.25 ± 0.75	2.4	5.4 ± 1.8	2.45 ± 1.55
6	6.05 ± 2.25	2.6 ± 1.0	2.2	5.7 ± 2.2	2.6 ± 1.6
7	6.45 ± 2.15	2.75 ± 0.95	2.2	6.0 ± 2.1	2.45 ± 1.45
8	6.55 ± 1.85	2.8 ± 0.8	2.1	5.9 ± 1.7	2.2 ± 1.2
9	6.85 ± 1.75	2.95 ± 0.75	2.1	6.2 ± 1.6	2.0 ± 1.1
10	7.15 ± 1.75	3.05 ± 0.75	2.1	6.4 ± 1.6	1.9 ± 1.0
11	7.6 ± 2.0	3.25 ± 0.85	2.1	6.8 ± 1.8	1.8 ± 1.0
12	8.05 ± 2.15	3.45 ± 0.95	2.1	7.2 ± 2.0	1.75 ± 0.95

[a] 2-10 keV flux in units of 10^{-12} *ergs* $cm^{-2}s^{-1}$

[b] X-ray luminosity in the energy range 2-10 keV

[c] Units of 10^{45} *ergs* s^{-1}, calculated for $H_0 = 50 kms^{-1}Mpc^{-1}$, $q_0 = 0.5$

[d] Bolometric luminosity

[e] The iron line flux produced by the cluster assuming an Fe abundance of 0.2–0.4 solar, units of 10^{-5} *photons* cm^{-2} s^{-1}

Table 4: Ratio of measured to total cluster flux

Core Radius (arcminutes)	β	Ratio[a]
0.42	0.70	3.8
0.18	0.63	5.7
0.20	0.62	4.9
0.76	0.85	3.0
0.78	0.83	2.8

[a]The ratio of the total flux emitted by the cluster to that emitted between one and three arcminutes from the source centre. Ratios are shown for the best fit to the cluster radial profile and for the full range of allowed values (at 90% confidence).

Table 5: The cluster contribution to the 1987/1988 *Ginga* observation of the E 1821+643 system

$T_{cluster}$ (keV)	Cluster[a] cont. %	Cluster[b] (eV)	QSO[c] (eV)
3	11 ± 2	35 ± 15	202 ± 94
4	19 ± 6	63 ± 35	198 ± 119
5	26 ± 9	83 ± 52	199 ± 157
6	30 ± 11	88 ± 54	212 ± 181
7	32 ± 11	83 ± 49	228 ± 185
8	33 ± 9	75 ± 41	242 ± 176
9	34 ± 9	68 ± 37	262 ± 183
10	36 ± 9	58 ± 41	281 ± 190
11	38 ± 10	61 ± 34	291 ± 202
12	40 ± 11	59 ± 32	305 ± 213

[a]The percentage of the total observed 2–10 keV emission which is provided by the cluster

[b]The apparent equivalent width of the cluster Iron line

[c]The observed equivalent width of the iron line from the QSO after subtracting the cluster from the total spectrum.

7 FIGURES

Figure 1. Background subtracted spectra from K1-16 and E 1821+643 . The spectra were taken from a circular area of radius 30 arcseconds centred on each object. To remove the residual traces of the QSO and cluster from the white dwarf spectrum, the background was taken from a region at the same distance from the QSO as K1-16 but on the opposite side.

Figure 2. A smoothed image of the region around E 1821+643 , channel range 70–129. The centroid of the QSO, marked q, is RA $18^h21^m58^s.1$ Dec $+64°20'43''$ (equinox 2000.0). No emission is seen from the nearby white dwarf, marked w, at this energy. The contour levels are 0.25,0.4,0.6,1,2,10 counts per 7.5 x 7.5 arcsecond^2 pixel. The background level is 0.010 ± 0.001 counts per pixel.

Figure 3. Radial profile fits, at 1 keV, to the standard PSPC PSF (solid line) for (a) E 1821+643 observation 1 (b) E 1821+643 observation 2. The radial profile of PG 1426+015 is given in both diagrams for comparison (stars).

Figure 4. Confidence contours of the cluster profile fit to the first *ROSAT* observation.

Figure 5. The best fit model to the radial profile and the residuals.

Figure 6. The 2–10 keV flux from the cluster as a function of temperature. The allowed values lie within the shaded area bounded by the lower limit of the flux extrapolated from the Feb 1991 *ROSAT* observation and the upper limit to thermal emission from a cluster in the 1990 *Ginga* observation. All limits are at 90% confidence.

FIG. 1

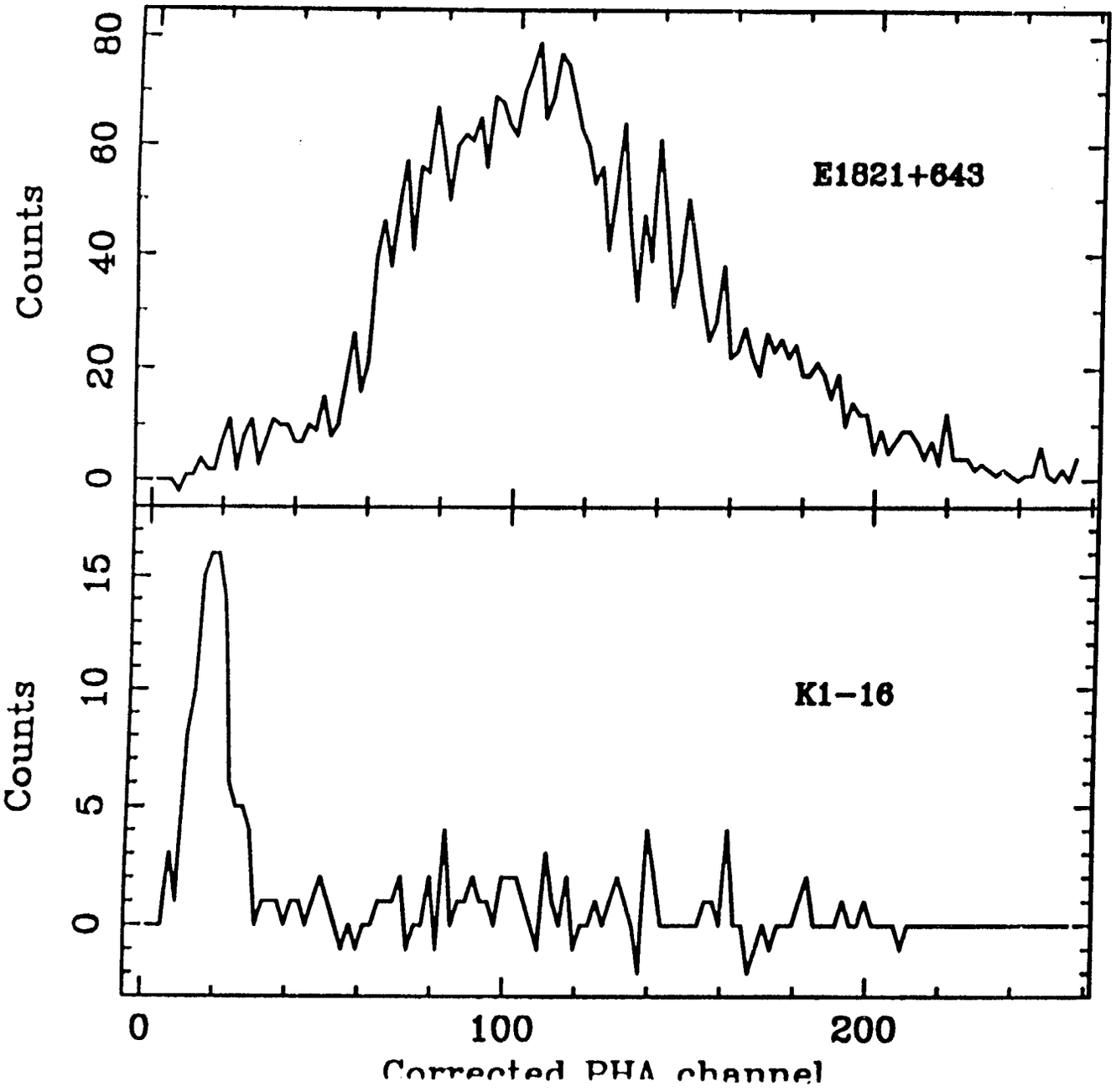
E1821+643
K1-16
Counts
Counts
0
20
40
60
80
0
5
10
15
0
100
200
Corrected PHA channel

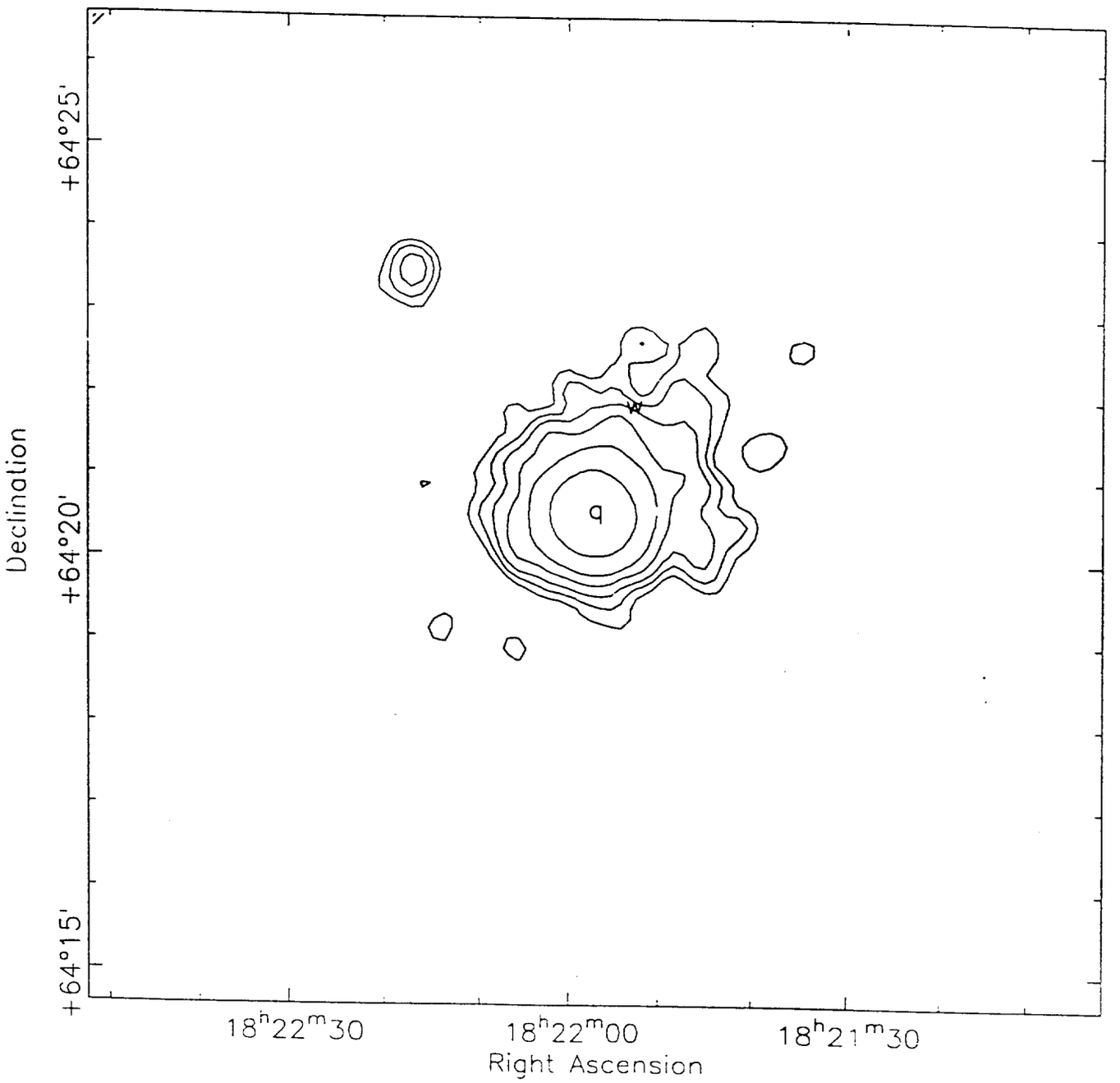
+64°25'
+64°20'
+64°15'
Declination
18h22m30
18h22m00
18h21m30
Right Ascension

FIG 2

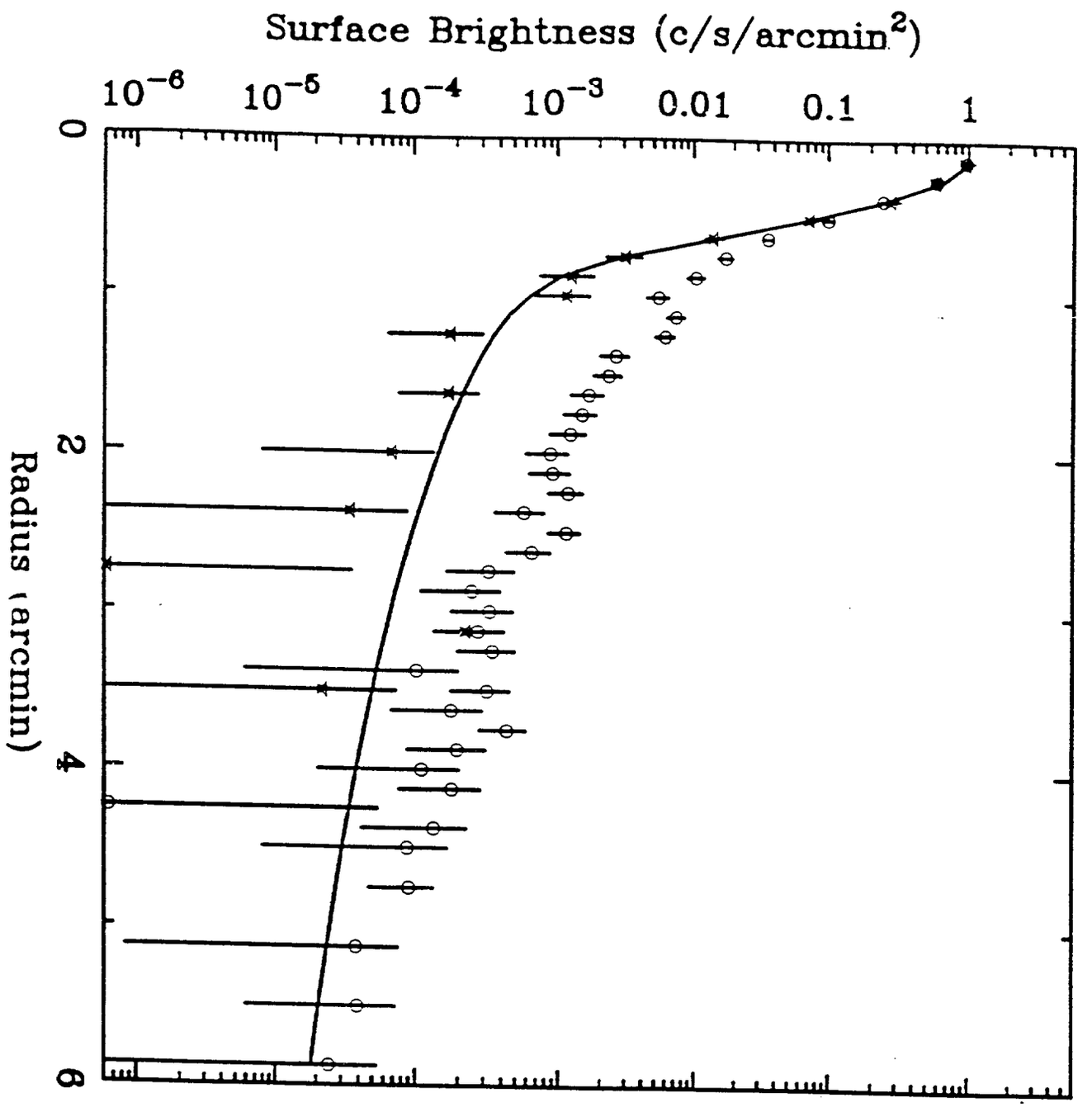
Surface Brightness (c/s/arcmin^2)
10^{-6}
10^{-5}
10^{-4}
10^{-3}
0.01
0.1
1
0
2
4
6
Radius (arcmin)

FIG 3a

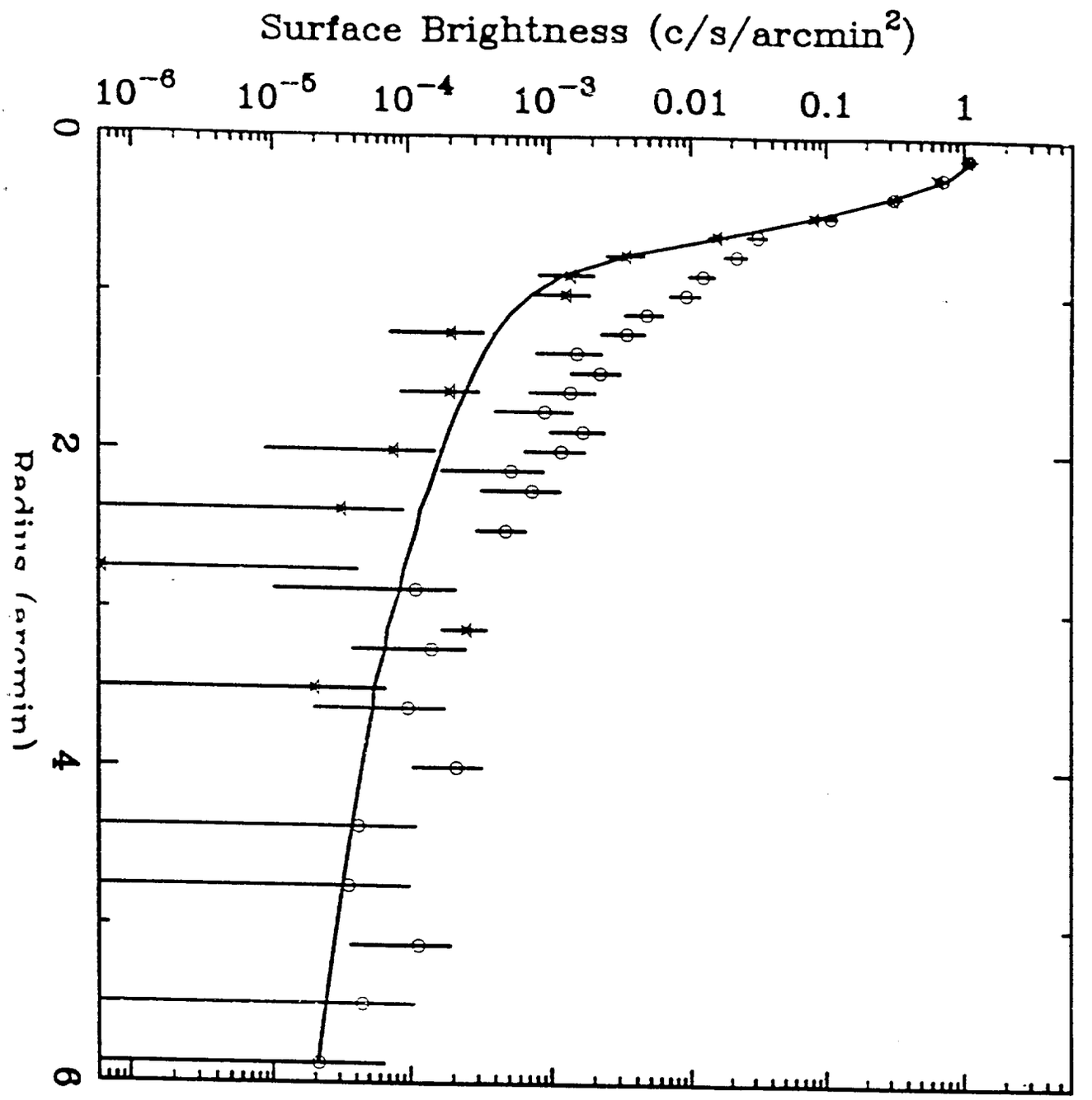
Surface Brightness (c/s/arcmin^2)
10^{-6}
10^{-5}
10^{-4}
10^{-3}
0.01
0.1
1
0
2
4
6
Radius (arcmin)

Fig 3B

FIG. 4

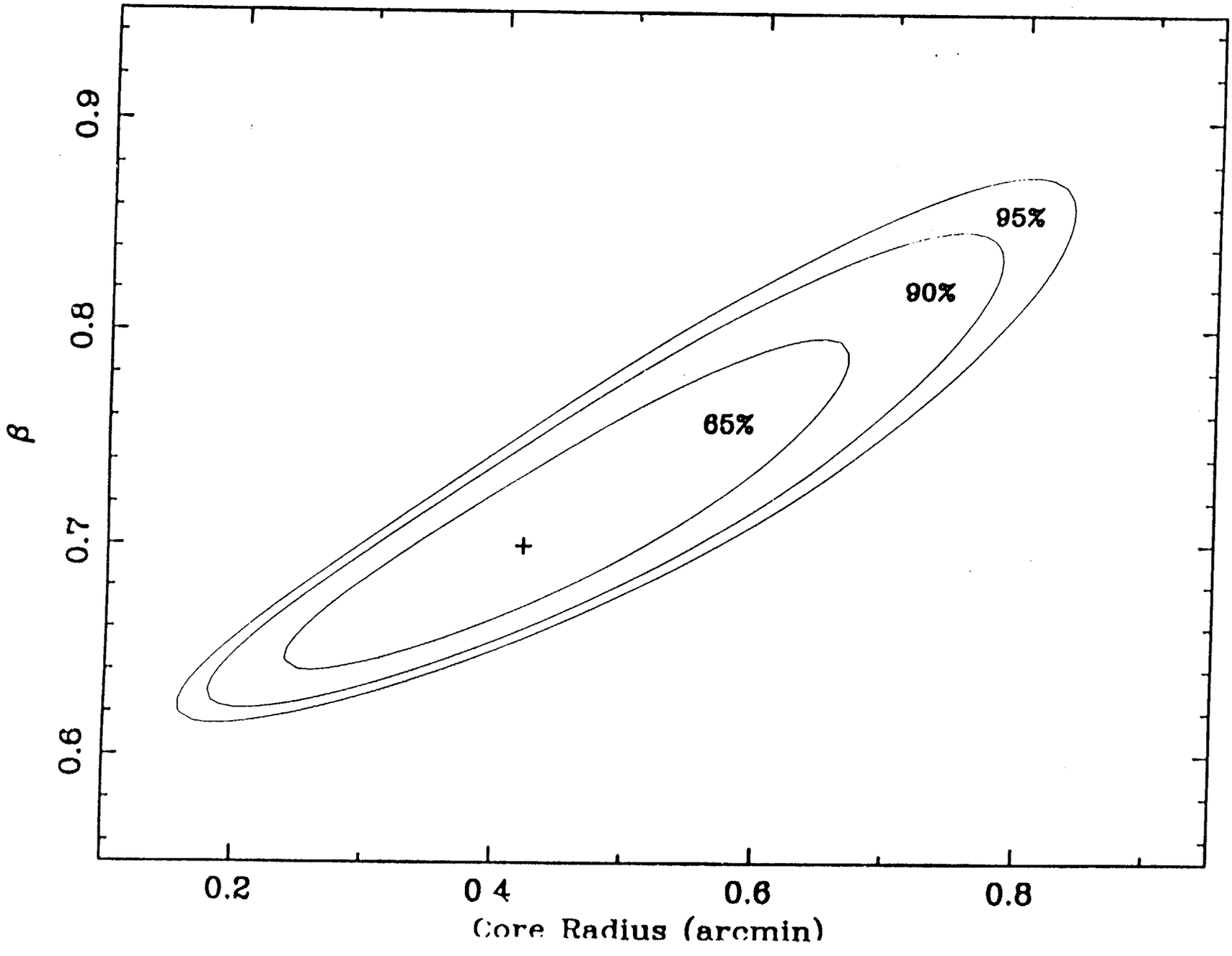

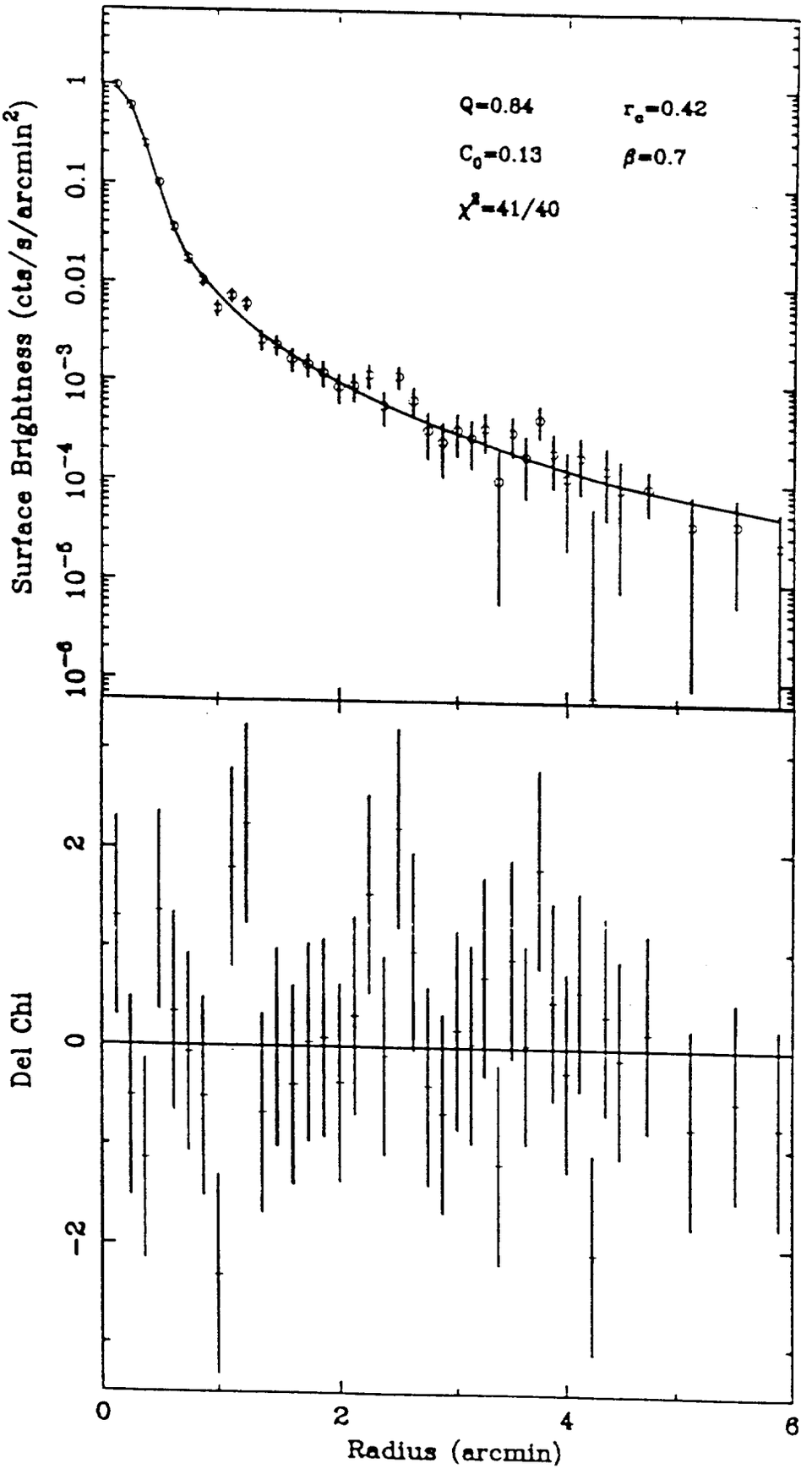
Q=0.84
r_c=0.42
C_0=0.13
β=0.7
χ^2=41/40
Surface Brightness (cts/s/arcmin^2)
1
0.1
0.01
10^{-3}
10^{-4}
10^{-5}
10^{-6}
Del Chi
2
0
-2
0
2
4
6
Radius (arcmin)

FIG. 5

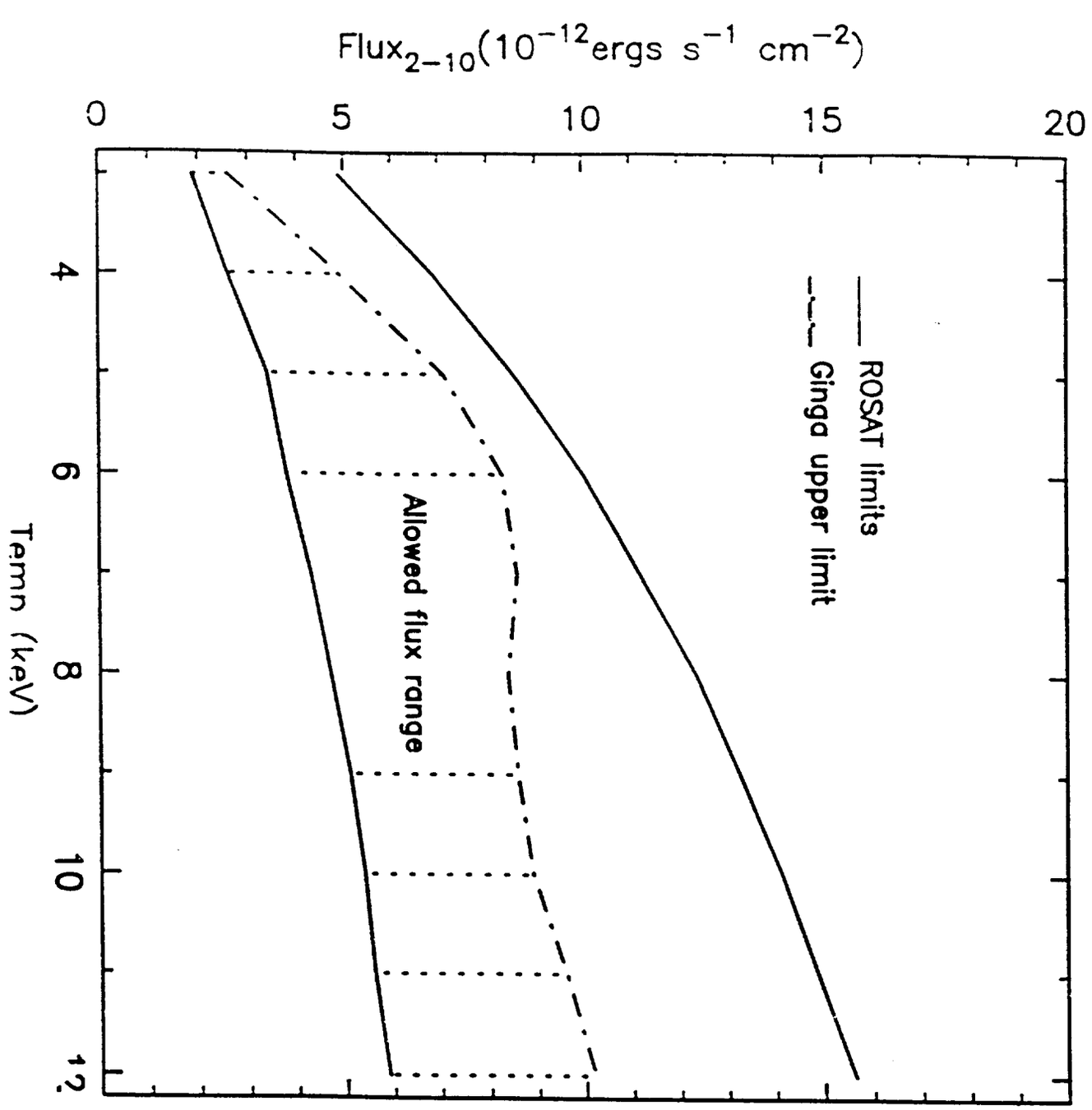
Flux$_{2-10}$(10^{-12}ergs s^{-1} cm^{-2})
0
5
10
15
20
4
6
8
10
12
Temp (keV)
ROSAT limits
Ginga upper limit
Allowed flux range

Fig 6